Modeling and Analysis of an Elastic Compound Strut in Axial Compression

Omer J. R, BSc (Hons), MSc, PhD, MILT, *Member, IAENG*

***Abstract*— This paper presents an analytical model for calculating the deformation behavior of an elastic, composite strut comprising any number of materials, which are represented by an assembly of concentric hollow cylinder. The model is applicable for pure axial compression for short struts provided elastic instability, if any, is assessed to be of negligible effect. For a typical constituent cylinder, relationships are derived to describe the deformations along three cylindrical co-ordinate axes. Lateral interaction between adjacent cylinders is modeled based on the elastic theory, taking into account the equilibrium of individual cylinders and the elastic parameters: stress-strain modulus and Poisson's ratio. The relationships are expressed in matrix notation and a computer program is developed to enhance rapidity of analysis. To assess the validity of the model, the program is used to analyze test data from an instrumented, steel-encased reinforced concrete column which had previously been loaded under controlled conditions in a laboratory. It is shown that the calculated and measured deformations of the column, at specified co-ordinates and along three cylindrical directions, agree to within 5%. Therefore the validity of the model is demonstrated.**

***Index Terms*—Elastic parameters, Stresses in cylindrical co-ordinate systems.**

I. Introduction

According to published [1],[2] experimental evidence, both the Young's modulus and the Poisson's ratio of concrete vary with radius on a cross-section of a cylindrical specimen. Both of these quantities could be 1.5 times greater at the centre than at the periphery of a concrete column. In the case of the composite strut analyzed here, the problem is further complicated by the presence of an external steel casing.

In the present study, a mathematical model is developed to simulate the elastic behavior of a short composite strut, comprising steel, reinforced concrete and plain concrete. The strut was instrumented and subjected to compression testing in the laboratory. Displacements in the constituent materials were measured at selected radial distances from the centre of the short column, so that the variations in the values of elastic constants with position of measurement are taken into consideration. This provides an analytical capability that represents the composite nature of the column cross-section better than the technique of modular ratio and transformed area of concrete.

Dr J. R. Omer is a Research Scientist at the University of Glamorgan, Pontypridd, South Wales, CF37 1DL, United Kingdom. Telephone: +44 (0) 1443 482162; Fax: +44 (0) 1443 482169; e-mail: jromer@ glam.ac.uk.

In order to minimize the effects of elastic instability, it is determined that a 0.9m in diameter by 2m long composite column would be an appropriate specimen for testing under pure compression behavior. The diameter of 0.9m is chosen to be large enough to allow measurement of strains at different radial distances from the centroidal axis of the column. The height of 2m gives a low slenderness ratio while simultaneously allowing space for installing strain gauges at the column mid height, which is sufficiently away from the ends where stress concentrations would inevitably occur.

Strain gauges, of the vibrating wire type, and linear extensometers were installed in the column at selected known radial distances from the axis of the column. In the first compression test (test No.1) the short column was encased in a steel tube 10mm thick, which formed material number 1. Material number 2 was a 197mm thick annular zone of reinforced concrete (having 18 numbers of 32mm diameter high yield steel bars). Finally, material number 3 was a 253mm thick inner core of plain concrete. In the second compression test, the steel casing was cut out so that there were two remaining materials.

II. Development of the Numeral Model

A. Mathematical idealization of the column cross-section

Let the column cross-section be represented by a number of (say N), concentric hollow cylinders with different material properties. This is shown in Fig. 1. Let the dimensions and properties of the n^{th} cylinder be:

r_{n-1} = internal radius
r_n = external radius
E_n = Elastic modulus
ν_n = Poisson's ratio
A_n = Cross-sectional area.

For the innermost cylinder, n=1, and for the outermost, n=N. It is assumed that the deformation of the column comprises the deformations of the individual constituent cylinders. The following three loading stages are considered:

1) A unit applied longitudinal load,

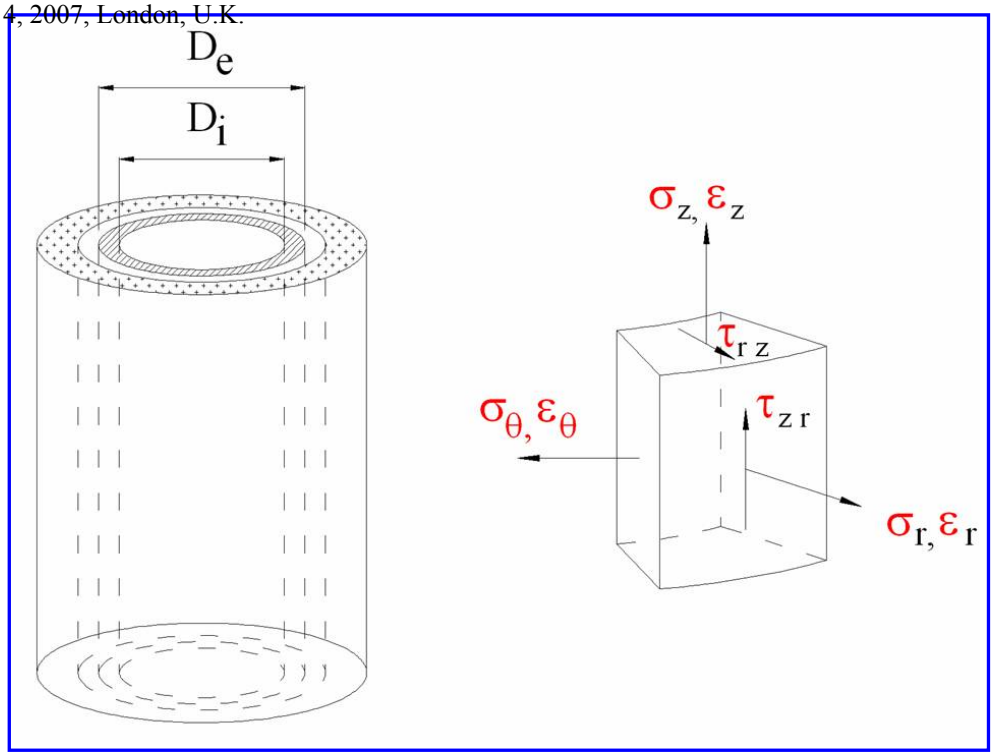

Fig. 1: Theoretical modeling of multi-material column as a number of concentric annuli

2) Artificially introduced lateral pressures on the contact surfaces of the cylinders to correct the incompatible radial displacements arising from load case (1) above, and

3) Superposition of above load cases to produce the final state of stress and deformation

The following assumptions are made:

(a) Each cylinder is free to displace radially in isolation.
(b) Load is applied and transmitted concentrically along the column.
(c) Shear stresses (τ_{rz} and τ_{zr} in Fig. 1) on boundary surfaces may be neglected.
(d) The material of each cylinder is linearly elastic and
(e) There is a small but essential cavity of radius r_o at the centre of the column (the cavity can be mathematically set to zero).

B. *Representation of stresses and strains*

Stresses and strains in the three cylindrical directions (z, *r*, θ) are considered (Fig. 1). Since loading is applied in the z-direction, it is assumed that the shear stresses τ_{rz} and τ_{zr} (on the *r*-θ and z-θ surfaces respectively) are negligible. In load case (1), elasticity relationships [3] from elementary mechanics are used to derive the axial, radial and circumferential stresses, $\sigma'_{nz}, \sigma'_{nr}, \sigma'_{n\theta}$ in the n^{th} cylinder due to unit applied axial load. Taking tensile stresses as positive, the stresses for load case (i) can be expressed in matrix form as follows:

$$\begin{Bmatrix} \sigma'_{nz} \\ \sigma'_{nr} \\ \sigma'_{n\theta} \end{Bmatrix} = \begin{Bmatrix} \dfrac{-1}{A_n + \dfrac{1}{E_n}\left(\sum_{i=1}^{n-1} A_i E_i + \sum_{i=n+1}^{N} A_i E_i\right)} \\ 0 \\ 0 \end{Bmatrix} \quad (1)$$

Therefore the resulting axial, radial and circumferential strains $\varepsilon'_{nz}, \varepsilon'_{nr}, \varepsilon'_{n\theta}$ in the n^{th} cylinder due to load case (i) are given by:

$$\begin{Bmatrix} \varepsilon'_{nz} \\ \varepsilon'_{nr} \\ \varepsilon'_{n\theta} \end{Bmatrix} = \frac{1}{E_n} \begin{bmatrix} 1 & -\nu_n & -\nu_n \\ -\nu_n & 1 & -\nu_n \\ -\nu_n & -\nu_n & 1 \end{bmatrix} \begin{Bmatrix} \sigma'_{nz} \\ \sigma'_{nr} \\ \sigma'_{n\theta} \end{Bmatrix} \quad (2a)$$

$$= \frac{1}{E_n}\begin{bmatrix} 1 & -\nu_n & -\nu_n \\ -\nu_n & 1 & -\nu_n \\ -\nu_n & -\nu_n & 1 \end{bmatrix} \begin{Bmatrix} \dfrac{-1}{A_n + \dfrac{1}{E_n}\left(\sum_{i=1}^{n-1} A_i E_i + \sum_{i=n+1}^{N} A_i E_i\right)} \\ 0 \\ 0 \end{Bmatrix} \quad \ldots(2b)$$

In load case (ii), let contact pressures p_{n-1} and p_n be imposed on the inner and outer surfaces of the n^{th} cylinder. For radial force equilibrium, the contact pressure on the outer surface of the $(n\text{-}1)^{th}$ cylinder must equal p_{n-1}. Similarly the pressure on the inner surface of the $(n+1)^{th}$ next cylinder must equal p_n. There is no pressure on the inner surface of the first cylinder as well as on the outer surface of the last cylinder.

The stresses induced at any radial co-ordinate r (measured from the centre of the column) within the n^{th} cylinder, may be derived from established formulae from the theory of "thick cylinders" [4]. Hence the axial, radial and circumferential stresses $\sigma''_{nz}, \sigma''_{nr}, \sigma''_{n\theta}$ in the n^{th} cylinder for load case (ii), which now vary with radial distance, are given by:

$$\begin{Bmatrix} \sigma''_{nz} \\ \sigma''_{nr} \\ \sigma''_{n\theta} \end{Bmatrix} = \begin{Bmatrix} 0 \\ -p_{n-1}A_n + p_n B_n \\ -p_{n-1}A_n + p_n C_n \end{Bmatrix} \quad (3a)$$

where

$$\left.\begin{aligned} A_n &= \left(\frac{r_{n-1}^2}{r_n^2 - r_{n-1}^2}\right)\left(1 - \frac{r_n^2}{r^2}\right) \\ B_n &= \left(\frac{r_n^2}{r_n^2 - r_{n-1}^2}\right)\left(1 - \frac{r_{n-1}^2}{r^2}\right) \\ C_n &= \left(\frac{r_n^2}{r_n^2 - r_{n-1}^2}\right)\left(1 + \frac{r_{n-1}^2}{r^2}\right) \end{aligned}\right\} \quad (3b)$$

The ensuing strains $\varepsilon''_{nz}, \varepsilon''_{nr}, \varepsilon''_{n\theta}$ are again given in terms of the stresses and elastic constants as follows:

$$\begin{Bmatrix} \varepsilon''_{nz} \\ \varepsilon''_{nr} \\ \varepsilon''_{n\theta} \end{Bmatrix} = \frac{1}{E_n}\begin{bmatrix} 1 & -\nu_n & -\nu_n \\ -\nu_n & 1 & -\nu_n \\ -\nu_n & -\nu_n & 1 \end{bmatrix} \begin{Bmatrix} \sigma''_{nz} \\ \sigma''_{nr} \\ \sigma''_{n\theta} \end{Bmatrix} \quad (4)$$

$$= \frac{1}{E_n}\begin{bmatrix} 1 & -\nu_n & -\nu_n \\ -\nu_n & 1 & -\nu_n \\ -\nu_n & -\nu_n & 1 \end{bmatrix} \begin{Bmatrix} 0 \\ -p_{n-1}A_n + p_n B_n \\ -p_{n-1}A_n + p_n C_n \end{Bmatrix} \quad (5)$$

The stresses and strains in load cases (i) and (ii) can be superimposed, since the problem is assumed to be linearly elastic. So the final stresses1 $\sigma_{nz}, \sigma_{nr}, \sigma_{n\theta}$ for the n^{th} cylinder are defined as follows:

$$\begin{Bmatrix} \sigma_{nz} \\ \sigma_{nr} \\ \sigma_{n\theta} \end{Bmatrix} = \begin{Bmatrix} \sigma'_{nz} \\ \sigma'_{nr} \\ \sigma'_{n\theta} \end{Bmatrix} + \begin{Bmatrix} \sigma''_{nz} \\ \sigma''_{nr} \\ \sigma''_{n\theta} \end{Bmatrix} = \begin{Bmatrix} \dfrac{-1}{A_n + \dfrac{1}{E_n}\left(\sum_{i=1}^{n-1} A_i E_i + \sum_{i=n+1}^{N} A_i E_i\right)} \\ -p_{n-1}A_n + p_n B_n \\ -p_{n-1}A_n + p_n C_n \end{Bmatrix} \quad (6)$$

Similarly, the final strains $\varepsilon_{nz}, \varepsilon_{nr}, \varepsilon_{n\theta}$ in the n^{th} cylinder are given by:

$$\begin{Bmatrix} \varepsilon_{nz} \\ \varepsilon_{nr} \\ \varepsilon_{n\theta} \end{Bmatrix} = \begin{Bmatrix} \varepsilon'_{nz} \\ \varepsilon'_{nr} \\ \varepsilon'_{n\theta} \end{Bmatrix} + \begin{Bmatrix} \varepsilon''_{nz} \\ \varepsilon''_{nr} \\ \varepsilon''_{n\theta} \end{Bmatrix} \quad (7)$$

C. Boundary conditions to be satisfied

The final state of stress and strain may be applied to satisfy the boundary conditions for force equilibrium and displacement compatibility. Once these conditions are satisfied, the cylinders are "assembled" to form the final state of stress and deformation of the column.

1) At the outside surface of the outermost cylinder (i.e the N^{th} cylinder), the pressure is atmospheric. Hence the net radial stress there is zero, thus

$$\left(\sigma_{Nr}\right)_{r=\frac{D}{2}} = 0 \quad (8)$$

where D= column diameter.

2) The radial stresses at the interfaces of the cylinders must be in equilibrium. Consider the n^{th} and the $(n+1)^{th}$ cylinders. Let

the radial stress at the outside face of the n[th] cylinder be $\left(\sigma_{nr}\right)_{outside}$ while that at the inside face of the $(n+1)^{th}$ cylinder be $\left(\sigma_{(n+1)r}\right)_{inside}$. For equilibrium, we have

$$\left(\sigma_{(n+1)r}\right)_{inside} = \left(\sigma_{nr}\right)_{outside} \quad (9)$$

3) For compatibility of radial displacements at boundaries, the radial displacement of the outer surface of the n^{th} cylinder must equal the radial displacement of the inner surface of the $(n+1)^{th}$ cylinder. Hence

$$\left(u_{nr}\right)_{outside} = \left(u_{(n+1)r}\right)_{inside} \quad (10)$$

4) Assuming that there is a small cavity at the centre of the column (the radius r_o of which can be mathematically set to zero), the radial stress at the inner surface of the first cylinder is zero, hence

$$\left(\sigma_{1r}\right)_{r=r_o} = 0 \quad (11)$$

D. Solution of the stresses and strains

Equation 10 may be considered in a slightly different form by expressing boundary radial displacements in terms of circumferential strains. The circumferential strain at the outer surface of the n[th] cylinder is given by

$$\left(\varepsilon_{n\theta}\right)_{outside} = \frac{\left(u_{nr}\right)_{outside}}{r_{outside}} \quad (12)$$

The circumferential strain at the inner surface of the $(n+1)^{th}$ can be expressed in a similar way. Therefore, the necessary and sufficient condition for displacement compatibility at boundaries is for the corresponding hoop strains to match. In addition, equating hoop strains rather than radial displacements eliminates the need for an integration process. For N number of cylinders, there are (N-1) boundaries. Thus, there will be (N-1) equations of compatibility containing an equal number of unknown radial pressures. These pressures can then be solved if the material properties are known.

III. APPLICATION OF THE MODEL TO A TRI-ANNULAR MATERIAL (STEEL-ENCASED, REINFORCED CONCRETE COLUMN)

In order to represent accurately the loaded behavior of the short column and to account for the variation of elastic properties with radial distance, a three-annulus configuration was proposed. The steel-encased column is divided into concentric cylinders of three materials as shown in Fig. 2.

(a) an inner core of plain concrete,
(b) a zone of reinforced concrete, and
(c) the steel casing.

There is also a central cavity which is mathematically set to "zero". For stress and strain predictions for the column tested without steel casing, there are only two constituent cylinders. Parallel with the load test, the foregoing method has been used to calculate the deformations of the column.

The elastic modulus of steel and concrete were determined from laboratory tests on samples as 205kN/mm^2 and 38kN/mm^2 respectively. The Poisson's ratio for steel and plain concrete were taken as 0.3 [5] and 0.2 [6] respectively. The elastic modulus value for the reinforced concrete zone is initially estimated using an "equivalent area" approach, which gives a value of 43kN/mm^2. Therefore, trial values of Poisson's ratio for reinforced concrete are then taken in the range 0.15-0.4.

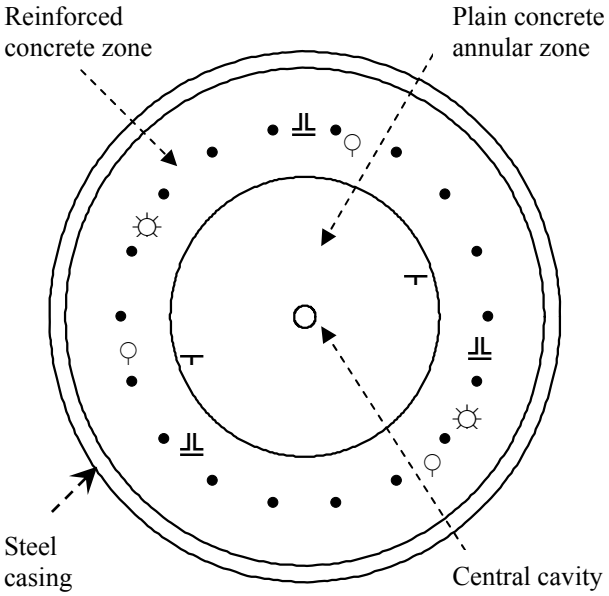

Legend: ♀Extensometers, ⩩Axial strain gauges, ☼Circumferential strain gauges, ⊤Radial strain gauges, ●Steel reinforcing bars .

Fig. 2: Representation of the composite steel-encased column by 3 concentric cylinders

Graphs of applied load versus the average axial (average of extensometer value ε_{z1} and vibrating wire strain gauge value ε_{z2}), radial (ε_r) and circumferential (ε_θ) strains were plotted from the results of both tests 1 (tri-material steel-encased column) and 2 (no casing and hence a two-material column). The gradients of the graphs represent strain per unit (1 kN) applied load and are called "normalized strains". The normalized strain values from all the gauges are presented in Tables 1 (test no. 1) and 2 (test no. 2). The normalized strain values shown have been calculated by linear regression on at least 15 test data points.

	Test 1-column with 10mm steel casing			
	ε_{z1}	ε_{z2}	ε_r	ε_θ
Cycle 1				
Loading	33.64	29.90	7.95	8.96
Unloading	33.17	27.58	7.95	8.53
Cycle 2				
Loading	29.63	28.21	7.95	7.26
Unloading	27.38	27.87	7.95	7.26
Cycle 3				
Loading	29.85	27.81	7.78	7.31
Unloading	28.88	26.63	7.78	7.74
Mean	30.43	28.00	7.89	7.39
Calculated	31.41		7.74	7.35

Table 1: Measured and calculated strains (x 10^{-9}) per kN applied load – test no. 1

	Test 2-column without steel casing			
	ε_{z1}	ε_{z2}	ε_r	ε_θ
Cycle 1				
Loading	35.45	30.35	8.60	8.20
Unloading	34.79	30.45	8.36	8.35
Cycle 2				
Loading	35.45	30.66	8.58	8.24
Unloading	35.12	30.56	8.49	8.31
Cycle 3				
Loading	35.85	30.42	8.63	8.37
Unloading	35.47	30.89	8.40	8.44
Mean	35.36	30.56	8.51	8.32
Calculated	38.44		8.38	8.80

Table 2: Measured and calculated strains (x 10^{-9}) per kN applied load – test no. 2

A back analysis process was devised to assess the elastic constants from actual measured strains. The procedure involved determining the influence of selected E and ν values, of the plain and reinforced concrete annuli, on the predicted axial, radial and circumferential strains. In all trial cases, the following values were kept constant: {E_s=205,000 N/mm^2, ν_s=0.3, ν_c=0.2} subscripts *s* and *c* refer to steel and concrete annuli respectively. Various incremental values of the elastic constants E_c, E_b and ν_b (subscript *b* refers to the reinforced concrete annulus) were input into a purpose written computer program so that stresses and strains could be generated at required increments of radius. It was also imperative to generate the strain values at radial co-ordinates corresponding to the locations of the embedded strain gauges.

The results of this parametric study are summarized in Table 3, which represents the closest match between calculated and measured strain values in all three directions. The measured strains are compared with the theoretically calculated strains listed at the bottom of the Tables 1 and 2. It is seen that the predicted strains are accurate to within 5% of the measured values and are remarkably consistent throughout.

Constituent material	Elastic modulus (kN/mm^2)	Poisson's ratio
Steel casing (*r*=450-460mm)	205	0.30
Stiffened concrete zone (*r*=253-450mm)	42	0.25
Plain concrete core (*r*=0-253 mm)	38	0.20

Table 3: Appropriate values of E and ν for constituent materials of the test column

IV. CONCLUSIONS

A mathematical model was successfully developed for elastic analysis of a compound column comprising any number annuli having different elastic parameters. Using the model, the material characteristics of the composite reinforced concrete short column were assessed accurately. The stiffening effect of steel on concrete has been realistically assessed by projecting the effective elastic modulus and Poisson's ratio of the reinforced zone of concrete at a given cross-section. The validity of the model was demonstrated by comparing predicted strains with measured values in three mutually perpendicular directions. An excellent agreement, to within 5% was observed between the measured and the predicted strain values at several locations. The results indicate the following:

a) The change in material properties due to reinforcing of concrete was found to affect the effective Poisson's ratio more than the Young's modulus.

b) For a specific amount of reinforcement, it was found that the Poisson's ratio of concrete increased by 25% whilst the Young's modulus increased by 10.5%.

c) There was demonstrated evidence that the elastic constants for plain concrete were position sensitive, which support previous observations by other researchers. The evidence arose from the fact that lower strain values were recorded near the central axis of the column. This suggested that there was compression of concrete centrally.

ACKNOWLEDGMENT

The author is grateful to the University of Glamorgan Directorate and to the Head of Faculty of Advanced Technology for supporting the research in terms of facilities and technical staff. Special appreciation is due to Cardiff County Council for permitting the unlimited use of their field test and for providing the initial research funding. The Building Research Establishment, Hertfordshire, UK, is thanked for their collaborative input in installing and monitoring the instrumentation used in the load testing the composite column.

REFERENCES

[1] S. A. Klink, “Actual Elastic Modulus of Concrete”, Technical Paper, American Concrete Institute - A.C.I. Journal. 82-54, 1985, pp630-633.
[2] S. A. Klink, “Actual Elastic Modulus of Concrete”, Technical Paper, American Concrete Institute - A.C.I. Journal. 82-54, 1985, pp813-817.
[3] S. P. Timoshenko, and J. M. Gere, “Mechanics of materials”, D.Van Nostrand Co., 1972, pp19-20.
[4] E. P. Popov, “Mechanics of materials”, 2nd Edition, Prentice- Hall Inc., 1976, pp562.
[5] British Standards Institution, “BS5950: 1990, Part 1 - Structural Use of Steelwork in Buildings”, 1990. Milton Keynes, England.
[6] British Standards Institution, “BS 8110, Part 1 - Structural Use of concrete", 1985, pp 2/3. Milton Keynes, England